

# Mechanism of $\beta$ -Hydrogen Elimination from Square Planar Iridium(I) Alkoxide Complexes with Labile Dative Ligands

Jing Zhao, Heather Hesslink, and John F. Hartwig\*

Contribution from the Department of Chemistry, Yale University, P.O. Box 208107, New Haven, Connecticut 06520-8017

Received February 16, 2001

**Abstract:** Mechanistic studies were conducted on  $\beta$ -hydrogen elimination from complexes of the general formula  $[\text{Ir}(\text{CO})(\text{PPh}_3)_2(\text{OR})]$ , which are square planar alkoxo complexes with labile ligands. The dependence of rate, isotope effect, and alkoxide racemization on phosphine concentration revealed unusually detailed information on the reaction pathway. The alkoxo complexes were remarkably stable, including those with a variety of electronically and sterically distinct groups at the  $\beta$ -carbon. These complexes were much more stable than the corresponding alkyl complexes. Thermolysis of these complexes in the presence of  $\text{PPh}_3$  yielded the iridium hydride  $[\text{Ir}(\text{CO})(\text{PPh}_3)_3\text{H}]$  and the corresponding aldehyde or ketone with rate constants that were affected little by the groups at the  $\beta$ -carbon. The reactions were first order in iridium complexes. At low  $[\text{PPh}_3]$ , the reaction rate was nearly zero order in  $\text{PPh}_3$ , but reactions at high  $[\text{PPh}_3]$  revealed an inverse dependence of reaction rate on  $\text{PPh}_3$ . The rate constants were similar in toluene, THF, and chlorobenzene. The  $y$ -intercept of a  $1/k_{\text{obs}}$  vs  $[\text{PPh}_3]$  plot displayed a primary isotope effect, indicating that the  $y$ -intercept did not simply correspond to phosphine dissociation. These data and a dependence of alkoxide racemization on  $[\text{PPh}_3]$  showed that the elementary  $\beta$ -hydrogen elimination step was reversible. A mechanism involving reversible  $\beta$ -hydrogen elimination followed by associative displacement of the coordinated ketone or aldehyde by  $\text{PPh}_3$  was consistent with all of our data. This mechanism stands in contrast with the pathways proposed recently for alkoxide  $\beta$ -hydrogen elimination involving direct elimination, protic catalysts, or binuclear mechanisms and shows that alkoxide elimination can follow pathways similar to those for  $\beta$ -hydrogen elimination from alkyl complexes.

## Introduction

$\beta$ -Hydrogen elimination and migratory insertion<sup>1,2</sup> are common elementary reactions in both homogeneous and heterogeneous catalysis. Extensive mechanistic studies have been conducted on  $\beta$ -hydrogen elimination from transition metal alkyl complexes.<sup>1</sup> These mechanistic studies have revealed a common reaction pathway that requires an open coordination site and a transition state involving a syn coplanar arrangement of the  $\alpha$ - and  $\beta$ -carbons, the  $\beta$ -hydrogen, and the metal center. This transition state generates an olefin hydride complex, which often generates the final product after olefin dissociation.

$\beta$ -Hydrogen elimination from a metal alkyl and the microscopic reverse of this reaction occurs in a variety of catalytic processes including dehydrogenation of alkanes,<sup>3–6</sup> Mizoroki–Heck olefination,<sup>7</sup> olefin isomerization,<sup>8</sup> cycloisomerizations,<sup>9</sup> and hydroformylation of internal olefins to  $n$ -aldehydes.<sup>10–12</sup>

The microscopic reverse of this reaction is olefin insertion into a metal hydride, which occurs in olefin hydrogenation.<sup>13</sup>  $\beta$ -Hydrogen elimination from a metal alkyl must be suppressed to observe cross-coupling<sup>14</sup> of main group alkyl reagents with vinyl and aryl electrophiles.

$\beta$ -Hydrogen elimination from alkoxo and amido complexes and the microscopic reverse of this reaction are similarly involved in catalytic processes. These processes include transfer hydrogenations using alcohol reducing agents<sup>15–17</sup> and cycloisomerizations involving aldehydes.<sup>18</sup> The microscopic reverse of this reaction is involved in aldehyde, ketone, and imine hydrogenation.<sup>16,19,20</sup>  $\beta$ -Hydrogen elimination from alkoxo complexes must be avoided if aromatic etherification is to encompass alcohol substrates that bear a methylene or methine

(1) Cross, R. J. In *The Chemistry of the Metal–Carbon Bond*; Hartley, F. R., Patai, S., Eds.; John Wiley: New York, 1985; Vol. 2, pp 559–624.

(2) Collman, J. P.; Hegedus, L. S.; Norton, J. R.; Finke, R. G. In *Principles and Applications of Organotransition Metal Chemistry*, 2nd ed.; University Science Books: Mill Valley, 1987; pp 383–388.

(3) Crabtree, R. H.; Mellea, M. F.; Mihelcic, J. M.; Quirk, J. M. *J. Am. Chem. Soc.* **1982**, *104*, 107–113.

(4) Felkin, H.; Fillebeen-Khan, T.; Gault, Y.; Holmes-Smith, R.; Zakrzewski, J. *Tetrahedron Lett.* **1984**, *25*, 1279–1282.

(5) Liu, F.; Pak, E. B.; Singh, B.; Jensen, C. M.; Goldman, A. S. *J. Am. Chem. Soc.* **1999**, *121*, 4086–4087.

(6) Liu, F. C.; Goldman, A. S. *Chem. Commun.* **1999**, 655–656.

(7) Crisp, G. T. *Chem. Soc. Rev.* **1998**, *27*, 427–436.

(8) For a recent example see: Wakamatsu, H.; Nishida, M.; Adachi, N.; Mori, M. *J. Org. Chem.* **2000**, *65*, 3966–70 and references therein.

(9) Trost, B. M.; Krische, M. J. *Synlett* **1998**, 1–16.

(10) Collman, J. P.; Hegedus, L. S.; Norton, J. R.; Finke, R. G. In *Principles and Applications of Organotransition Metal Chemistry*, 2nd ed.; University Science Books: Mill Valley, 1987; p 622.

(11) van der Veen, L. A.; Kamer, P. C. J.; van Leeuwen, P. *Angew. Chem. Int. Ed. Engl.* **1999**, *38*, 336–338.

(12) Breit, B.; Winde, R.; Harms, K. *J. Chem. Soc.* **1997**, 2681–2682.

(13) Collman, J. P.; Hegedus, L. S.; Norton, J. R.; Finke, R. G. In *Principles and Applications of Organotransition Metal Chemistry*, 2nd ed.; University Science Books: Mill Valley, 1987; p 523.

(14) Hegedus, L. S. *Transition Metals in the Synthesis of Complex Organic Molecules*; University Science Books: Mill Valley, CA, 1994.

(15) Uematsu, N.; Fujii, A.; Hashiguchi, S.; Ikariya, T.; Noyori, R. *J. Am. Chem. Soc.* **1996**, *118*, 4916–4917.

(16) Noyori, R.; Hashiguchi, S. *Acc. Chem. Res.* **1997**, *30*, 97–102.

(17) Mestroni, G.; Zassinovich, G.; Camus, A.; Martinelli, F. *J. Organomet. Chem.* **1980**, *198*, 87–96.

(18) Montgomery, J. *Acc. Chem. Res.* **2000**, *33*, 467–473.

(19) Palmer, M. J.; Wills, M. *Tetrahedron: Asymmetry* **1999**, 2045–2061.

(20) James, B. R. *Chem. Ind.* **1995**, *62*, 167–180.

hydrogen  $\alpha$  to oxygen.<sup>21,22</sup> Despite being common steps of catalytic processes, direct observations of  $\beta$ -hydrogen elimination from alkoxo and amido complexes are much less common than those from alkyl complexes,<sup>23–29</sup> and  $\beta$ -hydrogen elimination from alkoxo complexes is not well defined mechanistically.

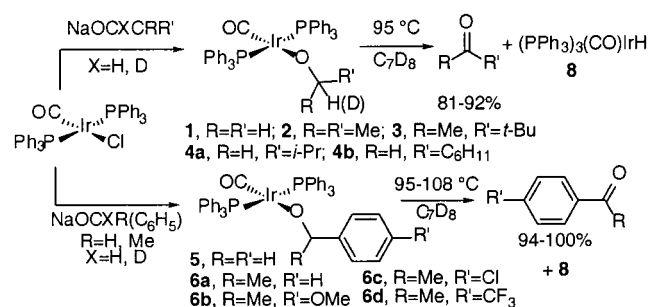
Evidence for  $\beta$ -hydrogen elimination from alkoxides is indirect in most cases. Yet, a few mechanistic studies have been conducted on isolated alkoxo complexes that cleanly generate aldehyde or ketone and metal hydride product, and in each case the mechanism has been proposed or shown to be distinct from the conventional mechanism for  $\beta$ -hydrogen elimination from alkyls. In one case, alkoxo  $\beta$ -hydrogen elimination from a 16-electron square planar complex [(DPPE)Pt(OMe)<sub>2</sub>] occurred.<sup>28</sup> This reaction was faster than  $\beta$ -hydrogen elimination from classic platinum dialkyls with the same ligand. It was proposed that an 18-electron aldehyde hydride complex is formed as an intermediate. However, chelation of the phosphine prevented detailed data on possible ligand dissociation paths. Partial dissociation of the chelating phosphine is generally undetectable by kinetic studies.

More detailed mechanistic data have been obtained on  $\beta$ -hydrogen elimination from saturated Ir(III) alkoxo complexes, and these studies revealed unusual mechanisms.<sup>23,26,27</sup> In two cases the reaction occurred in the presence of added alcohol,<sup>23,27</sup> and the order of the reaction in added alcohol was positive and noninteger. Thus, the authors could not pinpoint a transition state that contains the number of methanol groups in the experimental rate equation, but proposed a structure with hydrogen bonding involving a variable number of alcohols. The other example of  $\beta$ -hydrogen elimination from an Ir(III) alkoxo complex involved a dinuclear transition state formed from catalytic amounts of an iridium triflate.<sup>26</sup>

One study of rhenium alkoxo complexes probed  $\beta$ -hydrogen elimination indirectly.<sup>30</sup> In this case, the data supported a mechanism that is similar to the typical one for  $\beta$ -hydrogen elimination from alkyl complexes. [Cp\*Rh(NO)(PPh<sub>3</sub>)OR] catalyzed the racemization of alcohols, and this racemization was proposed to occur by  $\beta$ -hydrogen elimination of the rhenium alkoxo. The rate of racemization depended inversely on phosphine concentration. This information implied that  $\beta$ -hydrogen elimination was preceded by phosphine dissociation and that the phosphine dissociation allowed formation of an aldehyde hydride complex. This species provided the diastereomeric alkoxo complex by reinsertion.

Complexes containing a square planar geometry with labile dative ligands are common structures in catalytic processes. In contrast to data on the  $\beta$ -hydrogen elimination from alkoxo complexes with the geometries of the above examples, data on  $\beta$ -hydrogen elimination from alkoxo complexes with a square planar geometry and labile dative ligands are scarce. To test whether these complexes would show mechanisms for  $\beta$ -hy-

## Scheme 1



drogen elimination that are similar to those of the 18-electron Ir(III) complexes or to those of classic square planar alkyl complexes, we studied alkoxo complexes based on the Vaska fragment. Atwood had reported previously some of the alkoxo complexes we used for the study. He had shown that they were isolable and would generate iridium hydride upon thermolysis.<sup>31</sup> Moreover, we had recently provided some mechanistic data on  $\beta$ -hydrogen elimination from related amido complexes,<sup>24</sup> allowing comparisons between the mechanism for  $\beta$ -hydrogen elimination from alkoxo and amido complexes.

We report our results from this study, which provided an unusually detailed reaction path for the  $\beta$ -hydrogen elimination. This pathway involves a reversible, elementary  $\beta$ -hydrogen elimination step. An unexpected influence of phosphine concentration on reaction rate and racemization of the alkoxo complex uncovered the reversibility of this step. The isotope effect on the  $y$ -intercept of a plot correlating  $1/k_{\text{obs}}$  with phosphine concentration also revealed this reversibility.

## Results

**1. Synthesis and Thermolysis of Vaska-Type Alkoxo Complexes.** The synthesis and thermolysis of Vaska-type alkoxo complexes are summarized in Scheme 1. The isopropoxide was prepared previously by Atwood,<sup>31,32</sup> who first showed that it underwent  $\beta$ -hydrogen elimination. In our hands, sodium alkoxides reacted with Vaska's complex within an hour in THF solvent to form stable, monomeric, terminal alkoxo or benzyloxo complexes bearing  $\beta$ -hydrogens in 46–84% yield. Enantiopure (*R*)-**6a** was prepared by a one-pot procedure involving reaction of the alcohol and Vaska's complex in the presence of NaH in THF solvent.

Thermolysis of these complexes occurred smoothly in the presence of added PPh<sub>3</sub> in aromatic solvents between 95 and 108 °C to form the ketone or aldehyde and [Ir(CO)(PPh<sub>3</sub>)<sub>3</sub>H].<sup>33</sup> No reaction of the product hydride with the starting alkoxo<sup>31</sup> occurred in dry solvents. The organic products were identified by <sup>1</sup>H NMR and mass spectroscopy, as well as by GC or HPLC retention times.

Experiments involving thermolysis of the alkoxo in the presence of a ketone that is different from the product ketone showed that the overall  $\beta$ -hydrogen elimination process was irreversible. <sup>2</sup>H, <sup>1</sup>H, and <sup>31</sup>P NMR spectroscopy showed that isopropoxide **2** and phenethoxide **6a** did not incorporate deuterated or protiated acetone, respectively, during the  $\beta$ -elimination at 80 and 110 °C. At the concentrations employed, we would be able to detect by <sup>2</sup>H and <sup>31</sup>P NMR spectroscopy

(21) Hartwig, J. F. *Angew. Chem., Int. Ed. Engl.* **1998**, *37*, 2046–2067.

(22) Wolfe, J. P.; Wagaw, S.; Marcoux, J.-F.; Buchwald, S. L. *Acc. Chem. Res.* **1998**, *31*, 805–818.

(23) Blum, O.; Milstein, D. *J. Am. Chem. Soc.* **1995**, *117*, 4582–4594.

(24) Hartwig, J. F. *J. Am. Chem. Soc.* **1996**, *118*, 7010–7011.

(25) Hartwig, J. F.; Richards, S.; Baranano, D.; Paul, F. *J. Am. Chem. Soc.* **1996**, *118*, 3626–3633.

(26) Ritter, J. C. M.; Bergman, R. G. *J. Am. Chem. Soc.* **1998**, *120*, 6826–6827.

(27) Blum, O.; Milstein, D. *J. Organomet. Chem.* **2000**, *593–594*, 479–484.

(28) Bryndza, H. E.; Calabrese, J. C.; Marsi, M.; Roe, D. C.; Tam, W.; Bercaw, J. E. *J. Am. Chem. Soc.* **1986**, *108*, 4805–4813.

(29) Fryzuk, M. D.; Piers, W. E. *Organometallics* **1990**, *9*, 986–988.

(30) Saura-Llamas, I.; Gladysz, J. A. *J. Am. Chem. Soc.* **1992**, *114*, 2136–2144.

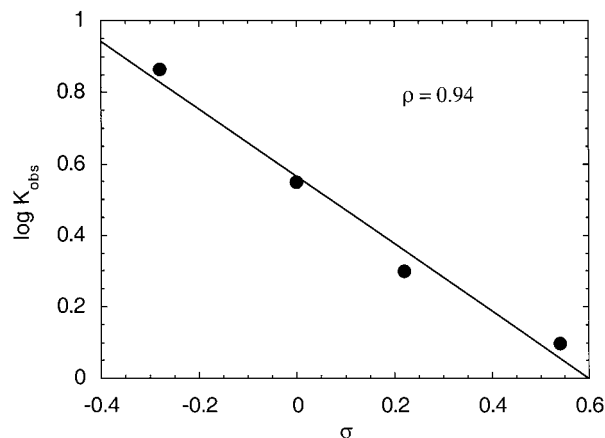
(31) Atwood, J. D.; Bernard, K. A.; Rees, W. M. *Organometallics* **1986**, *5*, 390–391.

(32) Rees, W. M.; Churchill, M. R.; Fettingner, J. C.; Atwood, J. D. *Organometallics* **1985**, *4*, 2179–2185.

(33) Ahmad, N.; Robinson, S. D.; Uttley, M. F. *J. Chem. Soc., Dalton Trans.* **1972**, 843–847.

**Table 1.** Structural Effects on the Rate Constants at 95 °C for  $\beta$ -Hydrogen Elimination from Ir(I) Alkoxo Complexes<sup>a</sup>

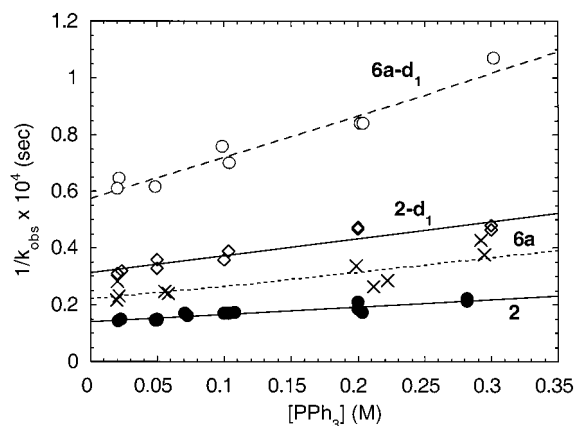
Complex	$k_{\text{obs}} \times 10^4 \text{ (s}^{-1}\text{)}$	Complex	$k_{\text{obs}} \times 10^4 \text{ (s}^{-1}\text{)}$
[Ir]-OMe (1)	2.1	[Ir]-O-  (4b)	3.5
[Ir]-O-  (2)	1.9	[Ir]-O-  (5)	2.6
[Ir]-O-  (3)	3.0	[Ir]-O-  (6a)	1.5
[Ir]-O-  (4a)	2.2		

<sup>a</sup> [Ir] = [*trans*-Ir(CO)(PPh<sub>3</sub>)<sub>2</sub>].**Figure 1.** Hammett plot for  $\beta$ -hydrogen elimination from **6a–d**. Cpd,  $k_{\text{obs}} \times 10^4$ : **6a**, 3.5; **6b**, 7.3; **6c**, 2.0; **6d**, 1.2.

10% of the exchanged product and by <sup>1</sup>H NMR 5% or less of the exchanged product.

The series of alkoxo complexes revealed a surprising lack of dependence of reaction rate on the steric and electronic properties at the  $\beta$ -hydrogen of the alkoxide. The  $k_{\text{obs}}$  values are provided in Table 1. These data show less than a factor of 3 difference in rate for benzyloxo vs alkoxo and for methoxo vs hindered alkoxo complexes. Although compound **6a** reacted more slowly than **5**, suggesting that a substituent on the  $\beta$ -carbon retards the reaction, compound **2** reacted with nearly the same rate constant as compound **1**, suggesting that this effect is subtle if present at all. One trend that was consistent, however, was the observation of slightly faster rates when increased steric hindrance was present about the  $\gamma$ -carbon. For example, compound **3** reacted faster than compound **2**, and compound **4b** reacted faster than **4a**. Qualitative studies on solvent effects showed similar rates in toluene, THF, and chlorobenzene.

The effect of electron density at the  $\beta$ -position was revealed by a Hammett analysis of  $\beta$ -phenethoxide complexes **6a–d**. The reaction rates measured by <sup>1</sup>H NMR spectroscopy under conditions of a large excess of added PPh<sub>3</sub> (vide infra) demonstrated that electron-withdrawing substituents decreased the reaction rate, and a Hammett plot (Figure 1) showed a  $\rho$ -value of  $-0.94$ . This effect can be rationalized in several ways: by greater stability of the resulting electron-rich ketone complex and concomitant transition state stabilization for the C–H bond cleavage, by reduced stability of the electron-rich starting benzyloxo complex, or by migration of the hydrogen with partial hydridic character. A  $\pi$ -bound complex of an electron-poor ketone, which might be the product formed initially from the elimination, should be more, rather than less, stable than that of an electron-rich ketone. This effect has been

**Figure 2.** Plot of  $1/k_{\text{obs}}$  vs [PPh<sub>3</sub>] for protiated and deuterated versions of **2** and **6a**. Reactions were conducted at 110 °C.**Table 2.** Dependence of Alkoxide Racemization on [PPh<sub>3</sub>]

starting ee (%)	[PPh <sub>3</sub> ] (M)	conversion (%)	ee (%) after conversion
84	0.3	40	84
84	0.3	75	81
>95	0.02	20	64
>95	0.02	40	18
>95	0.02	80	17

observed previously by Gladysz for ketone complexes of rhenium<sup>34,35</sup> and argues against the first explanation. However, the ketone complex that is formed first could be  $\eta^1$ -bound and would then be more stable when the ketone is more electron rich. Concerning the difference in ground-state energies controlling the reaction rates, the differences in thermodynamic stability of these phenethoxide complexes should be small.<sup>36</sup> Yet the differences in transition state energies that account for these rate differences are also small. Thus, this explanation cannot be ruled out without firm thermodynamic data. The third explanation is most conventional, however, and would be consistent with hydridic character for the electron-rich iridium product.

**2. Mechanistic Studies.** The influence of added phosphine on the overall reaction rate and on the degree of racemization of the enantiopure phenethoxide complex (*R*)-**6a** was used to reveal the precise reaction pathway. The rate constants for reaction of **2** and **6a** were measured in C<sub>7</sub>D<sub>8</sub> with added [PPh<sub>3</sub>-*d*<sub>15</sub>] ranging from 0.02 to 0.30 M. The reactions were clearly first order in the iridium alkoxide.

The dependence of  $1/k_{\text{obs}}$  on added [PPh<sub>3</sub>-*d*<sub>15</sub>] is shown in Figure 2. Within a conventional range of small amounts of added [PPh<sub>3</sub>-*d*<sub>15</sub>], the reaction appeared to be zero order in free ligand. However, rate constants measured with a large increase in the concentration of added PPh<sub>3</sub>-*d*<sub>15</sub> showed a small but measurable decrease in  $k_{\text{obs}}$  upon increasing [PPh<sub>3</sub>-*d*<sub>15</sub>].

In a mechanistically revealing set of experiments, the degree of racemization of (*R*)-**6a** was shown to depend on the concentration of added PPh<sub>3</sub> (Table 2). For example, (*R*)-**6a** underwent little or no detectable racemization during reactions run at high concentrations of added PPh<sub>3</sub>-*d*<sub>15</sub>, but (*R*)-**6a** showed substantial racemization during reactions run at low [PPh<sub>3</sub>-*d*<sub>15</sub>]. An increase in racemized material was observed with increased

(34) Mendez, N. Q.; Seyler, J. W.; Arif, A. M.; Gladysz, J. A. *J. Am. Chem. Soc.* **1993**, *115*, 2323–2334.(35) Klein, D. P.; Dalton, D. M.; Mendez, N. Q.; Arif, A. M.; Gladysz, J. A. *J. Organomet. Chem.* **1991**, *412*, C7–C10.(36) Holland, P. L.; Andersen, R. A.; Bergman, R. G.; Huang, J. K.; Nolan, S. P. *J. Am. Chem. Soc.* **1997**, *119*, 12800–12814.

conversion. In these experiments, racemization was evaluated by first hydrolyzing the alkoxo complex and then analyzing the extruded alcohol by chiral stationary phase HPLC and chiral GC.

The deuterium isotope effect on the thermolysis of **2** and **6a** was also evaluated as a function of phosphine concentration. This measurement was conducted as a function of  $[\text{PPh}_3\text{-}d_{15}]$  because the kinetic importance of the C–H bond cleavage step depends on whether dissociation of  $\text{PPh}_3\text{-}d_{15}$  and  $\beta$ -hydrogen elimination are reversible. The reversibility of these steps may depend on  $[\text{PPh}_3\text{-}d_{15}]$ . The consequences of different reagent concentrations on observed kinetic isotope effects are often overlooked.

Figure 2 shows the dependence of the rate constant on  $[\text{PPh}_3\text{-}d_{15}]$  for reaction of **2** and **2-d<sub>1</sub>** and for reaction of **6a** and **6a-d<sub>1</sub>**. These data reveal a significant isotope effect on the y-intercept and slope of a plot of  $1/k_{\text{obs}}$  vs  $[\text{PPh}_3\text{-}d_{15}]$ . The isotope effect on the y-intercept was  $2.3 \pm 0.2$  for **2** and  $2.6 \pm 0.3$  for **6a**. The isotope effect on the slope was  $2.3 \pm 0.5$  for **2** and  $3.0 \pm 1.0$  for **6a**.

## Discussion

**1. Comparative Stability of Alkoxo, Amido, and Alkyl Complexes.** It was commonly believed that low-valent, late transition metal alkoxo complexes would have weak bonds due to an unfavorable hard–soft match between ligand and metal.<sup>37</sup> Thermodynamic studies showed that this prediction of homolytic bond strengths was unjustified and that metal alkoxo bond dissociation energies are often higher than those of metal alkyls.<sup>38</sup> However, some reaction pathways that are high in energy for metal alkyl complexes are low in energy for metal alkoxides. For example, the basic alkoxide nonbonded electrons can facilitate direct reaction at the alkoxo ligand or dissociation of ancillary ligands due to  $\pi$ -stabilization of the resulting unsaturated intermediate.<sup>39,40</sup> Moreover, the greater stability of alkoxide anions can induce bond heterolysis to generate reactive ion pairs with a metal cation and an alkoxo anion.

It is these properties that allow the unusual mechanisms for  $\beta$ -hydrogen elimination from Ir(III) alkoxo complexes noted in the Introduction to be more energetically accessible than they are for the analogous alkyl complexes. Yet, Bryndza's study of  $[(\text{DPPE})\text{Pt}(\text{OMe})(\text{Et})]$  showed that the alkyl group could be more reactive than the alkoxide toward  $\beta$ -hydrogen elimination within the same complex. Perhaps no late metal system shows as great a difference in stability of alkoxo vs alkyl complexes as the Vaska-type system reported here. Schwartz's group generated the analogous alkyl complexes at low temperature, and these complexes underwent  $\beta$ -hydrogen elimination near 0 °C. All of the alkoxo complexes prepared by Atwood and by us require hours to decompose at 80–110 °C. As will be discussed below, the mechanism for the  $\beta$ -hydrogen elimination is similar to that for late metal alkyl complexes. Yet,  $\beta$ -hydrogen elimination from the Vaska-type iridium complexes is much slower for the alkoxides than it is for the alkyls. Thus,  $\beta$ -hydrogen elimination of alkoxo and alkyl complexes of the same metal fragment may occur by a similar mechanism with the relative rate  $k_{\text{M-R}} \gg k_{\text{M-OR}}$ .

A comparison of the stability of the alkoxo complexes with the related amido complexes<sup>24</sup> shows that these classes of complexes undergo  $\beta$ -hydrogen elimination at similar rates. This similar rate for  $\beta$ -hydrogen elimination of square planar alkoxo and amido complexes that possess labile dative ligands has several consequences for catalytic processes. The slower rate for C–O bond-forming reductive elimination vs C–N reductive elimination, along with this similar rate for  $\beta$ -hydrogen elimination, explains the difficulty in developing catalytic systems that couple alcohols containing hydrogens  $\alpha$  to oxygen with unactivated aryl halides.<sup>41–44</sup> Second, the similar rates for  $\beta$ -hydrogen elimination suggest that for the opposite process, insertion, imines should be as reactive as ketones toward transition metal hydrides. Although rapid rates for ketone and imine hydrogenations have now been observed,<sup>45,46</sup> some rapid imine hydrogenations are proposed to occur by a pathway that bypasses imine insertion.<sup>47,48</sup> The faster rate for  $\beta$ -hydrogen elimination from alkyls implies that olefin insertion will be faster, and this assertion is consistent with the greater diversity of structures for olefin hydrogenation catalysts than imine or ketone hydrogenation catalysts.

**2. Mechanistic Studies.** Experimental data and previous thermodynamic studies rule out mechanisms involving CO dissociation for the  $\beta$ -hydrogen elimination. The most convincing argument against a pathway involving CO dissociation is based on previous measurements of Ir–CO bond energies for closely related compounds. These measured bond energies are between 72 and 84.4 kcal/mol, which are remarkably high for a dative ligand.<sup>49</sup> These values are 40–50 kcal/mol too high to allow CO to be a part of the reaction pathway for the observed  $\beta$ -hydrogen elimination.<sup>49</sup> In addition, thermolysis of the alkoxo complexes in the presence of CO led to the formation of carboalkoxy complexes, as described previously.<sup>32</sup> This result prevented our obtaining a reaction order in CO that would probe for CO dissociation. However, this result also suggests that carboalkoxy complexes would be formed, at least in small amounts, if CO dissociation did occur.

Instead, pathways involving alkoxide dissociation, direct  $\beta$ -hydrogen elimination, or initial phosphine dissociation are more likely. Six such pathways are shown in Scheme 2. All of the pathways shown would be first order in iridium alkoxide, but would differ in their dependence of reaction rate and degree of racemization on solvent and added  $[\text{PPh}_3]$ .<sup>50</sup>

Reaction by pathway A, involving alkoxide dissociation, would be zero order in added  $[\text{PPh}_3]$  and highly dependent on solvent polarity. Reaction by pathway B, involving direct  $\beta$ -hydrogen elimination, would be zero order in added phosphine, but relatively independent of solvent polarity. The stereochemistry of **6a** during reactions by either pathway would

(41) Mann, G.; Incarvito, C.; Rheingold, A. L.; Hartwig, J. F. *J. Am. Chem. Soc.* **1999**, *121*, 3224–3225.

(42) Shelby, Q.; Kataoka, N.; Mann, G.; Hartwig, J. F. *J. Am. Chem. Soc.* **2000**, *122*, 10718–10719.

(43) Torraca, K.; Kuwabe, S.; Buchwald, S. *J. Am. Chem. Soc.* **2000**, *122*, 12907–12908.

(44) Aranyos, A.; Old, D. W.; Kiyomori, A.; Wolfe, J. P.; Sadighi, J. P.; Buchwald, S. L. *J. Am. Chem. Soc.* **1999**, *121*, 4369–4378.

(45) Blaser, H.; Spindler, F. *Chimia* **1997**, *51*, 297–299.

(46) Spindler, F.; Pugin, B.; Blaser, H.-U. *Angew. Chem., Int. Ed. Engl.* **1990**, *29*, 558–559.

(47) Haack, K.-J.; Hashiguchi, S.; Fujii, A.; Ikariya, T.; Noyori, R. *Angew. Chem., Int. Ed. Engl.* **1997**, *36*, 285–288.

(48) Yamakawa, M.; Ito, H.; Noyori, R. *J. Am. Chem. Soc.* **2000**, *122*, 1466–1478.

(49) Rosini, G. P.; Liu, F.; Krogh-Jespersen, K.; Goldman, A. S.; Li, C.; Nolan, S. P. *J. Am. Chem. Soc.* **1998**, *120*, 9256–9266.

(50) Experiments were conducted with  $\text{PPh}_3\text{-}d_{15}$ , but for simplicity we state the effect of added  $\text{PPh}_3$ .

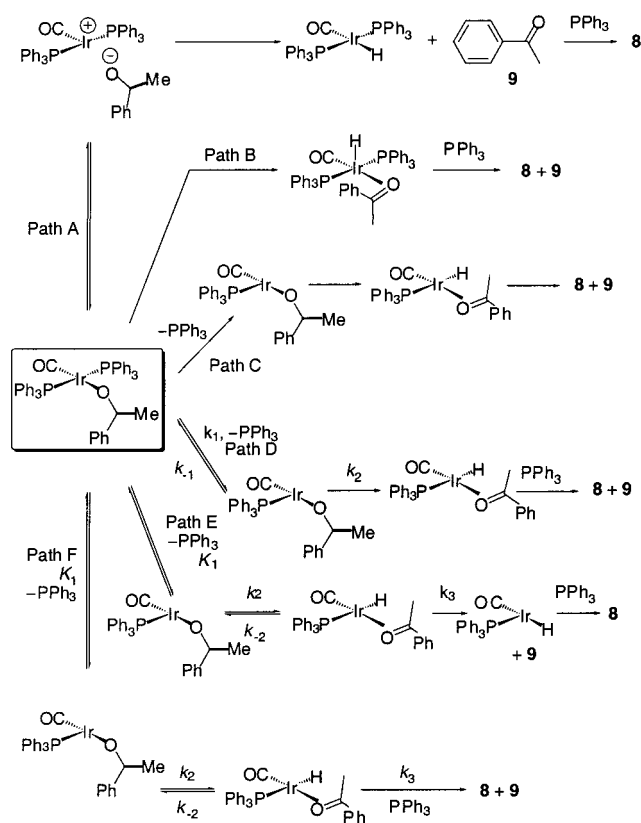
(37) Bryndza, H. E.; Tam, W. *Chem. Rev.* **1988**, *88*, 1163–1188.

(38) Bryndza, H. E.; Bercaw, J. E. *J. Am. Chem. Soc.* **1987**, *109*, 1444–1456.

(39) Glueck, D. S.; Bergman, R. G. *Organometallics* **1991**, *10*, 1479–1486.

(40) Bryndza, H. E.; Domaille, P. J.; Paciello, R. A.; Bercaw, J. E. *Organometallics* **1989**, *8*, 379–385.

Scheme 2



be independent of added  $\text{PPh}_3$ . Reaction by pathway C, involving irreversible phosphine dissociation, would exhibit no dependence of reaction rate or degree of racemization on  $[\text{PPh}_3]$ . Our data are not consistent with this set of predictions for paths A–C.

Pathway D, involving reversible phosphine dissociation and irreversible  $\beta$ -hydrogen elimination, would display an inverse first order dependence on  $[\text{PPh}_3]$ , at least at high  $[\text{PPh}_3]$  (eq 1). Although this dependence was observed, path D does not account for the observed racemization of (*R*)-**6a**.

Pathways E and F involve reversible phosphine dissociation and reversible  $\beta$ -hydrogen elimination. Path E involves dissociation of the final free ketone product in the last step, while path F involves associative substitution of phosphine for ketone in the final step. These two pathways show similar dependencies of  $k_{\text{obs}}$  on added  $[\text{PPh}_3]$  to that of path D. However, they do allow **6a** to undergo racemization because  $\beta$ -hydrogen elimination is reversible.

The rate equations corresponding to these reaction paths are provided in eq 1. The dependence of paths E and F on  $[\text{PPh}_3]$  is similar, but for different reasons. At low  $[\text{PPh}_3]$ , path E can be nearly zero order in added  $[\text{PPh}_3]$  because the  $\beta$ -hydrogen elimination step is much faster than recoordination of  $\text{PPh}_3$ . However, at high  $[\text{PPh}_3]$  the reaction can be strongly dependent on  $[\text{PPh}_3]$  because recoordination of phosphine is faster than  $\beta$ -hydrogen elimination and phosphine dissociation becomes reversible. Pathway F is also initiated by phosphine dissociation, but at low  $[\text{PPh}_3]$  reversible phosphine dissociation, reversible  $\beta$ -hydrogen elimination, and associative displacement of ketone by phosphine all occur. Because the phosphine is involved in both dissociative and associative steps before or during the irreversible step, a nearly-zero order dependence of  $k_{\text{obs}}$  on  $[\text{PPh}_3]$  is observed when  $[\text{PPh}_3]$  is low. At high  $[\text{PPh}_3]$ , the ketone is displaced more rapidly than it reinserts, and the

$\beta$ -hydrogen elimination is irreversible. Under these conditions, the phosphine is, therefore, involved only in a dissociative preequilibrium before the irreversible step of the reaction and the process is inhibited by added  $[\text{PPh}_3]$ .

$$d[\mathbf{6a}]/dt = k_{\text{obs}}[\text{Ir-OR}] \quad (1)$$

$$1/k_{\text{obs}} = -1/k_1 - k_{-1}[\text{PPh}_3]/(k_1k_2) \text{ for path D}$$

$$1/k_{\text{obs}} = -1/K_1k_2 - k_{-2}[\text{PPh}_3]/(K_1k_2k_3) \text{ for path E}$$

$$1/k_{\text{obs}} = -k_{-2}/(K_1k_2k_3) - [\text{PPh}_3]/(K_1k_2) \text{ for path F}$$

In addition to the ability to account for the alkoxide racemization, paths E and F, but not path D, account for the isotope effect on the  $y$ -intercept of the plot in Figure 2. For mechanisms E and F, the value of the  $y$ -intercept would contain the rate constant for  $\beta$ -hydrogen elimination and would show a primary isotope effect. In contrast, the  $y$ -intercept of a plot of  $1/k_{\text{obs}}$  vs  $[\text{PPh}_3]$  for mechanism D, involving irreversible  $\beta$ -hydrogen elimination, corresponds to the rate constant for ligand dissociation. Thus, the  $y$ -intercept would not display a significant isotope effect. The  $y$ -intercept of Figure 1 shows an isotope effect of  $2.3 \pm 0.2$  for reaction of **2** and  $2.6 \pm 0.3$  for reaction of **6a**. These data provide further evidence against pathway D and support pathway E or F. A comparison of the magnitudes of the isotope effect for the  $y$ -intercept ( $2.3 \pm 0.2$  for **2** and  $2.6 \pm 0.3$  for **6a**) and slope ( $2.3 \pm 0.5$  for **2** and  $3.0 \pm 1.0$  for **6a**) provides an approximate isotope effect for the insertion reaction. Assuming  $k_3$ , the replacement of coordinated ketone by phosphine, has no isotope effect, the ratio of the isotope effect for the  $y$ -intercept to the isotope effect for the slope provides the isotope effect for the insertion of ketone  $k_{-2}$ . This ratio is nearly 1. A similarly small isotope effect has been observed for some alkene insertions studied previously.<sup>51,52</sup>

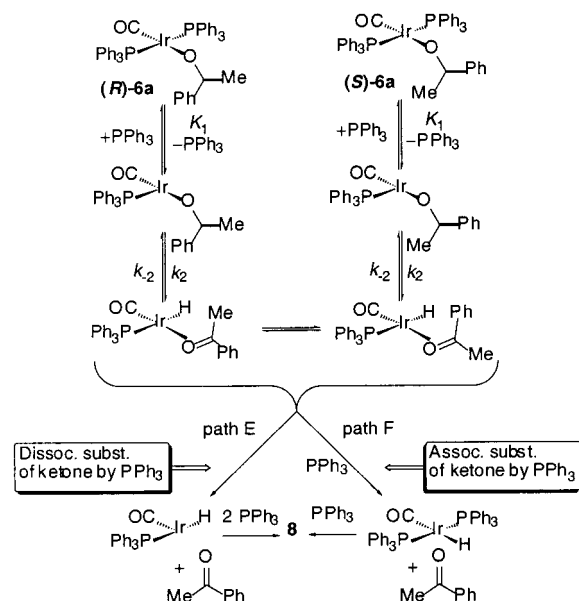
It remains to distinguish between pathways E and F. Although the reversibility of the  $\beta$ -hydrogen elimination in both pathways allows for racemization of **6a**, these mechanisms are clearly distinguished by the dependence of the degree of racemization on the concentrations of added  $\text{PPh}_3$ . As shown in Scheme 3, the concentration of  $\text{PPh}_3$  can influence the amount of racemization by altering the relative rates for reinsertion and for ketone displacement. In pathway E, increased concentrations of  $\text{PPh}_3$  will not affect the rate for reinsertion or dissociation of ketone because neither step involves reaction with this species. Thus, pathway E does not account for an influence of  $[\text{PPh}_3]$  on the rate of racemization of starting material.

However, pathway F, which involves associative displacement of ketone by  $\text{PPh}_3$ , predicts a dependence of the degree of racemization on  $[\text{PPh}_3]$ . The relative rates for the  $k_3$  and  $k_{-2}$  steps depend on  $[\text{PPh}_3]$  because  $k_3$  is associative. At high  $[\text{PPh}_3]$ , the associative displacement of ketone is faster than reinsertion, the  $\beta$ -hydrogen elimination becomes irreversible, and essentially no racemization of (*R*)-**6a** is observed. At low  $[\text{PPh}_3]$ , reinsertion of the ketone competes with its associative displacement, the  $\beta$ -hydrogen elimination is reversible, and racemization is observed. Thus, the observed dependence of the amount of racemization of **6a** on  $[\text{PPh}_3]$ , along with the apparent irreversible formation of free ketone, is inconsistent with pathway E and is consistent with pathway F.

(51) Doherty, N. M.; Bercaw, J. E. *J. Am. Chem. Soc.* **1985**, *107*, 2670–2682.

(52) Landis, C. R.; Hilfenhaus, P.; Feldgus, S. *J. Am. Chem. Soc.* **1999**, *121*, 8741–8754 and references therein.

Scheme 3



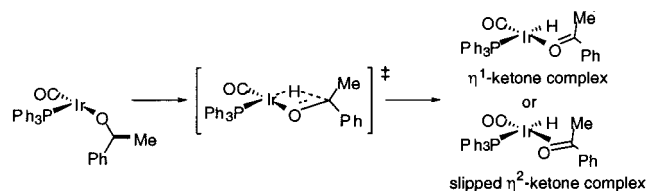
However, if path E were modified to include reversible dissociation of ketone and irreversible coordination of phosphine to the resulting 14-electron intermediate, then a dependence of racemization on  $[\text{PPh}_3]$  would be observed. If this pathway were followed, though, incorporation of free added ketone into the pool of alkoxide complex should have been observed. For example, reactions of isopropoxide **2** conducted in the presence of deuterated acetone and of phenoxide **6a** in the presence of protiated acetone should show formation of **2-d<sub>6</sub>** from **2** and **2** from **6a**. In neither case were detectable amounts of the exchange product observed. We estimated that the detection limit for ketone incorporation in these experiments would be 10% for reaction with deuterated acetone and 5% or less for formation of **2** from **6a**. Considering the large amount of racemization in the absence of  $\text{PPh}_3$ , the products from incorporation of free ketone must be larger than 5–10% of the alkoxide in solution if path E operates. Thus, pathway F is the only mechanism in Scheme 2 that is consistent with all of our data.

In addition to our experimental data, well-established mechanisms for ligand substitution favor pathway F over E. Square planar  $d^8$  complexes typically react by associative mechanisms, such as that in the last step of path F. Dissociative ligand substitution reactions of square planar compounds, such as the acetone complex in path E, are rare.<sup>53</sup>

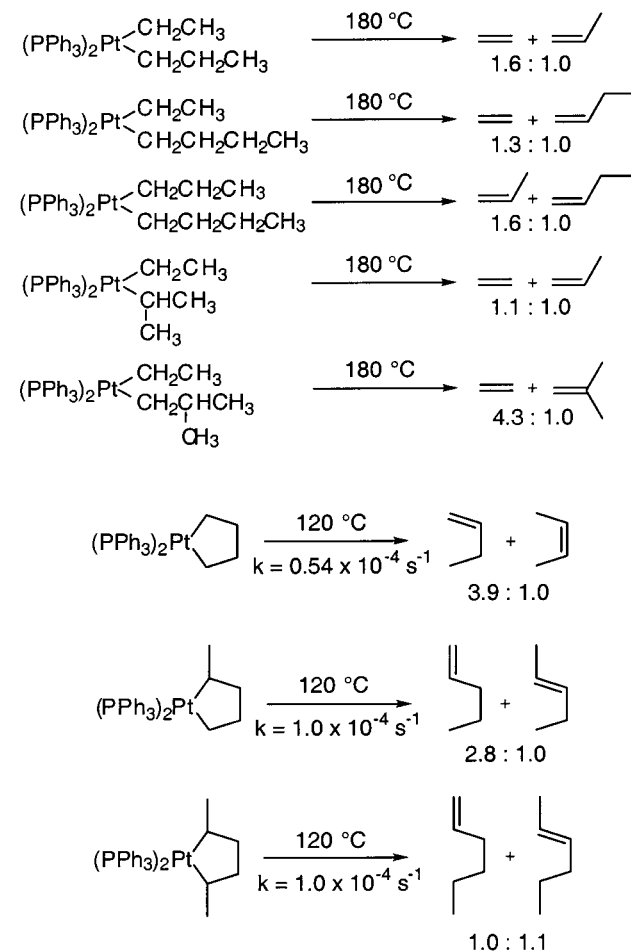
As has been emphasized in other systems previously,<sup>34,35,54</sup> the ketone complexes that are generated by  $\beta$ -hydrogen elimination from the Vaska-type alkoxide complexes are chiral. If racemization is to be observed, reinsertion must be preceded by rotation about the Ir–O bond if the ketone is bound  $\eta^1$  or migration of the metal from one ketone face to the other if the ketone is bound  $\eta^2$ . Thus, rotation about the Ir–O bond of an  $\eta^1$ -ketone complex,<sup>34</sup> or conversion of an  $\eta^2$ - to  $\eta^1$ -ketone complex and rotation about the Ir–O bond, must be similar to or greater than the rate for reinsertion.

**3. Mechanistic Implications of the Relative Stability of Alkoxo Complexes.** Only subtle differences in the rate constants for  $\beta$ -hydrogen elimination were observed as a function of large steric differences in the environment of the  $\beta$ -hydrogen. If the

Scheme 4



Scheme 5



reaction forms an  $\eta^2$ -ketone complex after  $\beta$ -hydrogen elimination, then, by the Hammond postulate, one might have expected the stability of the  $\eta^2$ -ketone to affect the overall reaction rate, and reactions that form less hindered ketones to occur faster. Moreover, aldehydes bind more tightly than ketones, suggesting that  $\beta$ -hydrogen eliminations that form aldehydes would be faster than those forming ketones. The direct formation of an  $\eta^1$ -aldehyde or ketone complex without an intermediate  $\eta^2$ -complex could explain the small steric effect we observe on reaction rate because the bulk of the coordinated carbonyl compound would be distal from the metal (Scheme 4).

By this logic,  $\beta$ -hydrogen elimination from alkyl complexes should show a greater steric effect than we observe here because the olefin in the olefin hydride intermediate must be bound  $\eta^2$ . Such trends for  $\beta$ -hydrogen elimination from isolated alkyl complexes have not been studied thoroughly, but we located two examples that probe the steric effect. Both examples showed a similar small dependence of the rate for  $\beta$ -hydrogen elimination on the steric properties of the alkyl group.<sup>55,56</sup> The examples at the top of Scheme 5 show that  $\beta$ -hydrogen elimination to form ethylene, propene, butene, and isobutylene all occur at similar rates. The examples at the bottom show that an

(53) Lanza, S.; Minniti, D.; Moore, P.; Sachinidis, J.; Romeo, R.; Tobe, M. *Inorg. Chem.* **1984**, *23*, 4428–4433.

(54) Klein, D. P.; Gladysz, J. A. *J. Am. Chem. Soc.* **1992**, *114*, 8710–8711.

intramolecular selectivity to form one of two olefins, one more substituted than the other, was again small. Perhaps the steric properties of the alkyl or alkoxide complexes are not dramatically different from those of the olefin or ketone complexes, the transition state is early, or the substituents favor the cyclic structure of the transition state, as in the well-known gem-dialkyl effect.<sup>57–59</sup>

Thus, the modest steric effects on the rates for  $\beta$ -hydrogen elimination from the alkoxo complexes have precedent in the  $\beta$ -hydrogen elimination from alkyl complexes. It is, therefore, unnecessary to invoke direct formation of an  $\eta^1$ -aldehyde or ketone complex to explain the small steric effect.

## Conclusions

A combination of phosphine dependence on stereochemical integrity, isotope effects on the  $y$ -intercept of a Lineweaver–Burk plot, and phosphine dependence on  $k_{\text{obs}}$  have clearly revealed a mechanism for  $\beta$ -hydrogen elimination that stands in contrast with the solvent-assisted ligand dissociation,<sup>23,27</sup> direct elimination,<sup>28</sup> and bimolecular hydride abstraction<sup>26</sup> deduced from previous studies. Instead, it is more akin to the classic  $\beta$ -hydrogen elimination from alkyl complexes.<sup>1</sup>

Further studies will be necessary to determine whether the more common pathway for  $\beta$ -hydrogen elimination of alkoxides will be the one outlined here and revealed by Gladysz in a different rhenium system or the pathways observed previously with saturated Ir(III) complexes. In either case, our studies show that an alkoxo complex need not be coordinatively saturated with tightly bound ligands to be stable. The alkoxo complexes studied here are far more stable than the analogous alkyls bearing  $\beta$ -hydrogens,<sup>60</sup> despite the open coordination site in the complex and its labile monodentate phosphines.

## Experimental Section

**General Methods.** Unless otherwise noted, all reactions, recrystallizations, and routine manipulations were performed at ambient temperature in a nitrogen-filled glovebox, or by using standard Schlenk techniques. Kinetic experiments were carried out in screw-capped NMR tubes in deuterated solvents and were monitored by  $^1\text{H}$  NMR spectroscopy. *n*-Pentane (tech grade) was distilled under nitrogen from purple sodium/benzophenone ketyl made soluble by addition of tetraglyme to the still. Benzene, toluene, tetrahydrofuran (THF), and diethyl ether were distilled from sodium/benzophenone ketyl under nitrogen. Deuterated solvents for use in NMR experiments were dried as their protiated analogues, but were vacuum transferred from the drying agent. Vaska's complex was prepared according to published methods. Triphenylphosphine was sublimed prior to use in kinetic experiments. All other chemicals were used as received from commercial suppliers.

$^1\text{H}$  and  $^{13}\text{C}$   $\{^1\text{H}\}$  NMR spectra were obtained on either a GE QE 300 MHz or a Bruker 400 MHz Fourier Transform spectrometer.  $^{31}\text{P}\{^1\text{H}\}$  and  $^2\text{H}$  NMR spectra were obtained on a GE  $\Omega$  300 or GE  $\Omega$  500 Fourier Transform spectrometer.  $^1\text{H}$ ,  $^{13}\text{C}$ , and  $^2\text{H}$  NMR chemical shifts are reported in parts per million downfield from tetramethylsilane and were referenced to residual protiated ( $^1\text{H}$ ) or deuterated solvent ( $^{13}\text{C}$ ) or natural abundance deuterated solvent ( $^2\text{H}$ ).  $^{31}\text{P}$  NMR chemical

shifts were referenced to 85%  $\text{H}_3\text{PO}_4$ . Elemental analyses were performed by Robertson Microlit Laboratories, Inc., Madison, NJ 07940 or Atlantic Microlab, Inc., Norcross, GA 30071. IR spectra were recorded on a MIDAC Fourier Transform spectrometer. GC analyses were conducted on a Hewlett-Packard 5890 instrument connected to a 3395 integrator. Enantiomeric excess was determined on a HPLC Chiralcel OD-H column (2% *i*-PrOH in hexane, 1 mL/min) or a GC Chiraldex B-PM column.

**General Procedure for the Preparation of Sodium Alkoxides.** Into a Schlenk flask was placed 300 mg of NaH (12.5 mmol). This solid was suspended in pentane. The flask was placed under nitrogen with stirring and was cooled with ice. The appropriate alcohol (15.0 mmol) was added into the flask using a 1 mL syringe. The solution started bubbling. The reaction mixture was allowed to warm to room temperature over the course of 3 h. After this time, the pentane was evaporated under vacuum. The resulting white powder was collected on a medium fritted funnel, washed with pentane, and was used without further purification.

**General Procedure for the Preparation of Iridium Alkoxides from Sodium Alkoxides.** Into a 20 mL vial was weighed 150 mg of Vaska's complex (0.192 mmol). This material was suspended in 10 mL of THF, and 1.2 equiv (0.230 mmol) of sodium alkoxide was added. The reaction was stirred at room temperature for 1 h. After this time, the THF was evaporated under reduced pressure. The resulting yellow film was dissolved in toluene, and the yellow suspension was filtered through Celite. The resulting solution was concentrated under vacuum, and crystallized by layering the concentrated toluene solution with pentane or ether and cooling at  $-35\text{ }^\circ\text{C}$ .

**General Procedure for the Preparation of Iridium Alkoxides from Sodium Hydride and Alcohols.** Into a 20 mL vial was weighed 150 mg of Vaska's complex (0.192 mmol). This material was suspended in 10 mL of THF, and 1.2 equiv (0.230 mmol) of sodium hydride was added. Then 1.5 equiv (0.288 mmol) of alcohol was added. The reaction was stirred at  $0\text{ }^\circ\text{C}$  for 1 h. After this time, the THF was evaporated under reduced pressure. The resulting yellow film was dissolved in toluene, and the yellow suspension was filtered through Celite. The resulting solution was concentrated under vacuum, and crystallized by layering the concentrated toluene solution with pentane or ether and cooling at  $-35\text{ }^\circ\text{C}$ .

***trans*-[Ir(PPh<sub>3</sub>)<sub>2</sub>](CO)(OMe) (1).** Following the general procedure involving alkoxide reagents, Vaska's complex (120 mg, 0.154 mmol) was combined with NaOMe (60.0 mg, 1.11 mmol) in THF. Workup and crystallization from toluene/pentane at  $-35\text{ }^\circ\text{C}$  gave yellow crystals of **1** (55 mg, 0.071 mmol, 46%).  $^1\text{H}$  NMR ( $\text{C}_6\text{D}_6$ ):  $\delta$  3.54 (s, 3H), 7.01–7.07 (m, 18H), 8.02 (m, 12H).  $^{31}\text{P}\{^1\text{H}\}$  NMR ( $\text{C}_6\text{D}_6$ ):  $\delta$  22.61.  $^{13}\text{C}\{^1\text{H}\}$  NMR ( $\text{C}_6\text{D}_6$ ):  $\delta$  60.58 (t,  $J = 3.8$  Hz), 128.35 (t,  $J = 4.9$  Hz), 130.17 (s), 133.67 (t,  $J = 25.7$  Hz), 135.18 (t,  $J = 6.4$  Hz), 175.36 (t,  $J = 10.7$  Hz). IR ( $\text{C}_6\text{D}_6$ ,  $\text{cm}^{-1}$ ): 1944 (s, CO).

***trans*-[Ir(PPh<sub>3</sub>)<sub>2</sub>](CO)(OCHMe<sub>2</sub>) (2).** Following the general procedure involving alkoxide reagents, Vaska's complex (146 mg, 0.185 mmol) was combined with NaOCHMe<sub>2</sub> (24.0 mg, 0.293 mmol) in THF. Workup and crystallization from toluene/pentane at  $-35\text{ }^\circ\text{C}$  gave yellow crystals of **2** (121 mg, 0.150 mmol, 81%).  $^1\text{H}$  NMR ( $\text{C}_6\text{D}_6$ ):  $\delta$  0.75 (d,  $J = 6.0$  Hz, 6H), 4.04 (sept,  $J = 5.6$  Hz, 1H), 7.01–7.10 (m, 18H), 8.03 (m, 12H).  $^{13}\text{C}\{^1\text{H}\}$  NMR ( $\text{C}_6\text{D}_6$ ):  $\delta$  29.23 (s), 73.64 (t,  $J = 5.9$  Hz), 128.17 (t,  $J = 4.7$  Hz), 130.14 (s), 133.78 (t,  $J = 25.2$  Hz), 135.31 (t,  $J = 6.0$  Hz), 176.06 (t,  $J = 11.6$  Hz).  $^{31}\text{P}\{^1\text{H}\}$  NMR ( $\text{C}_6\text{D}_6$ ):  $\delta$  24.19. IR ( $\text{C}_6\text{D}_6$ ,  $\text{cm}^{-1}$ ): 1943 (s, CO).

***trans*-[Ir(PPh<sub>3</sub>)<sub>2</sub>](CO)(OCDMe<sub>2</sub>) (2-*d*<sub>1</sub>).** Following the general procedure involving alkoxide reagents, Vaska's complex (153 mg, 0.196 mmol) was combined with NaOCDMe<sub>2</sub> (24.3 mg, 0.289 mmol) in THF. Workup and crystallization from toluene/pentane at  $-35\text{ }^\circ\text{C}$  gave yellow crystals of **2-*d*<sub>1</sub>** (127 mg, 0.158 mmol, 81%).  $^1\text{H}$  NMR ( $\text{C}_6\text{D}_6$ ):  $\delta$  0.74 (s, 6H), 7.01–7.11 (m, 18H), 8.03 (m, 12H).  $^{31}\text{P}\{^1\text{H}\}$  NMR ( $\text{C}_6\text{D}_6$ ):  $\delta$  24.20.  $^2\text{H}$  NMR ( $\text{C}_6\text{H}_6$ ):  $\delta$  3.97.

***trans*-[Ir(PPh<sub>3</sub>)<sub>2</sub>](CO)(OCHMeC(CH<sub>3</sub>)<sub>3</sub>) (3).** Following the general procedure involving alkoxide reagents, Vaska's complex (153 mg, 0.196 mmol) was combined with NaOCHMeC(CH<sub>3</sub>)<sub>3</sub> (34.6 mg, 0.279 mmol) in THF. Workup and crystallization from toluene/pentane at  $-35\text{ }^\circ\text{C}$  gave yellow crystals of **3** (132 mg, 0.156 mmol, 79%).  $^1\text{H}$  NMR ( $\text{C}_6\text{D}_6$ ):  $\delta$  0.60 (d,  $J = 6.0$  Hz, 3H), 0.70 (s, 9H), 3.60 (q,  $J = 5.7$  Hz,

(55) Komiya, S.; Yamamoto, A.; Yamamoto, T. *Chem. Lett.* **1978**, 1273–1276.

(56) McDermott, J. X.; White, J. F.; Whitesides, G. M. *J. Am. Chem. Soc.* **1976**, *98*, 6521–6528.

(57) Beesley, R. M.; Ingold, C. K.; Thorpe, J. F. *J. Chem. Soc.* **1915**, 107, 1080–1106.

(58) Capon, B.; McManus, S. P. In *Neighboring Group Participation*; Plenum: New York, 1976; pp 58–75.

(59) Lightstone, F. C.; Bruice, T. C. *J. Am. Chem. Soc.* **1996**, *118*, 2595–2605.

(60) Cannon, J. B.; Schwartz, J. *J. Am. Chem. Soc.* **1974**, *96*, 2276–2278.

1H), 7.01–7.11 (m, 18H), 8.00 (m, 12H).  $^{31}\text{P}\{\text{H}\}$  NMR ( $\text{C}_6\text{D}_6$ ):  $\delta$  23.36.  $^{13}\text{C}\{\text{H}\}$  NMR ( $\text{C}_6\text{D}_6$ ):  $\delta$  24.69 (s), 27.02 (s), 38.36 (s), 84.05 (t,  $J = 4.5$  Hz), 128.23 (t,  $J = 4.9$  Hz), 130.12 (s), 133.87 (t,  $J = 25.6$  Hz), 135.25 (t,  $J = 5.9$  Hz), 175.78 (t,  $J = 12.1$  Hz). IR ( $\text{C}_6\text{D}_6$ ,  $\text{cm}^{-1}$ ): 1936 (s, CO). Anal. Calcd for  $\text{C}_{43}\text{H}_{43}\text{P}_2\text{O}_2\text{Ir}$ : C, 61.04; H, 5.08. Found: C, 60.79; H, 5.24.

**trans-[Ir(PPh<sub>3</sub>)<sub>2</sub>](CO)(OCH<sub>2</sub>CH(CH<sub>3</sub>)<sub>2</sub>) (4a).** Following the general procedure involving alkoxide reagents, Vaska's complex (151 mg, 0.194 mmol) was combined with NaOCH<sub>2</sub>CH(CH<sub>3</sub>)<sub>2</sub> (28.0 mg, 0.292 mmol) in THF. Workup and crystallization from toluene/pentane at  $-35$  °C gave yellow crystals of **4a** (125 mg, 0.153 mmol, 79%).  $^1\text{H}$  NMR ( $\text{C}_6\text{D}_6$ ):  $\delta$  0.53 (d,  $J = 7.2$  Hz, 6H), 1.20 (nonet,  $J = 6.4$  Hz, 1H), 3.30 (d,  $J = 6.0$  Hz, 2H), 7.00–7.12 (m, 18H), 8.00 (m, 12H).  $^{31}\text{P}\{\text{H}\}$  NMR ( $\text{C}_6\text{D}_6$ ):  $\delta$  23.83.  $^{13}\text{C}\{\text{H}\}$  NMR ( $\text{C}_6\text{D}_6$ ):  $\delta$  19.54 (s), 34.03 (s), 80.45 (t,  $J = 3.3$  Hz), 128.32 (t,  $J = 5.6$  Hz), 130.17 (s), 133.72 (t,  $J = 25.7$  Hz), 135.23 (t,  $J = 7.0$  Hz), 175.73 (t,  $J = 10.4$  Hz). IR ( $\text{C}_6\text{D}_6$ ,  $\text{cm}^{-1}$ ): 1945 (s, CO). Anal. Calcd for  $\text{C}_{41}\text{H}_{39}\text{P}_2\text{O}_2\text{Ir}$ : C, 60.23; H, 4.77. Found: C, 60.51; H, 4.78.

**trans-[Ir(PPh<sub>3</sub>)<sub>2</sub>](CO)(OCH<sub>2</sub>(cyclohexyl)) (4b).** Following the general procedure involving alkoxide reagents, Vaska's complex (100 mg, 0.128 mmol) was combined with NaOCH<sub>2</sub>(cyclohexyl) (26.2 mg, 0.192 mmol) in THF. Workup and crystallization from toluene/pentane at  $-35$  °C gave yellow crystals of **4b** (68 mg, 0.079 mmol, 62%).  $^1\text{H}$  NMR ( $\text{C}_6\text{D}_6$ ):  $\delta$  0.57 (q,  $J = 11.2$  Hz, 2H), 0.86 (m, 1H), 1.00 (m, 3H), 1.26 (m, 2H), 1.57 (d,  $J = 9.6$  Hz, 3H), 3.38 (d,  $J = 5.2$  Hz, 2H), 7.02–7.12 (m, 18H), 8.00 (m, 12H).  $^{31}\text{P}\{\text{H}\}$  NMR ( $\text{C}_6\text{D}_6$ ):  $\delta$  23.82.  $^{13}\text{C}\{\text{H}\}$  NMR ( $\text{C}_6\text{D}_6$ ):  $\delta$  26.90 (s), 27.39 (s), 30.19 (s), 44.24 (s), 79.51 (t,  $J = 4.5$  Hz), 128.25 (t,  $J = 4.8$  Hz), 130.14 (s), 133.74 (t,  $J = 26.0$  Hz), 135.25 (t,  $J = 6.3$  Hz), 175.74 (t,  $J = 10.8$  Hz). IR ( $\text{C}_6\text{D}_6$ ,  $\text{cm}^{-1}$ ): 1944 (s, CO). Anal. Calcd for  $\text{C}_{44}\text{H}_{43}\text{P}_2\text{O}_2\text{Ir}$ : C, 61.62; H, 5.01. Found: C, 61.70; H, 5.04.

**trans-[Ir(PPh<sub>3</sub>)<sub>2</sub>](CO)(OCH<sub>2</sub>Ph) (5).** Following the general procedure involving alkoxide reagents, Vaska's complex (176 mg, 0.226 mmol) was combined with NaOCH<sub>2</sub>Ph (48.4 mg, 0.372 mmol) in THF. Workup and crystallization from toluene/pentane at  $-35$  °C gave yellow crystals of **5** (162 mg, 0.190 mmol, 84%).  $^1\text{H}$  NMR ( $\text{C}_6\text{D}_6$ ):  $\delta$  4.64 (s, 2H), 6.76–6.79 (m, 2H), 6.98–7.15 (m, 21H), 7.97–8.00 (m, 12H).  $^{31}\text{P}\{\text{H}\}$  NMR ( $\text{C}_6\text{D}_6$ ):  $\delta$  24.0.  $^{13}\text{C}\{\text{H}\}$  NMR ( $\text{C}_6\text{D}_6$ ):  $\delta$  74.98 (t, 3.0 Hz), 125.23 (s), 126.46 (s), 127.4 (s), 128.37 (s), 130.23 (s), 133.50 (t, 25.5 Hz), 135.15 (t, 6.0 Hz), 148.28 (s), 175.43 (t, 11.8 Hz). IR ( $\text{C}_6\text{D}_6$ ,  $\text{cm}^{-1}$ ): 1947 (s, CO). Anal. Calcd for  $\text{C}_{44}\text{H}_{37}\text{P}_2\text{O}_2\text{Ir}$ : C, 62.06; H, 4.35. Found: C, 62.20; H, 4.45.

**trans-[Ir(PPh<sub>3</sub>)<sub>2</sub>](CO)(OCHMePh) (6a).** Following the general procedure involving alkoxide reagents, Vaska's complex (201 mg, 0.258 mmol) was combined with NaOCHMePh (59.0 mg, 0.410 mmol) in THF. Workup and crystallization from toluene/pentane at  $-35$  °C gave yellow crystals of **6a** (170 mg, 0.196 mmol, 76%).  $^1\text{H}$  NMR ( $\text{C}_6\text{D}_6$ ):  $\delta$  0.89(d,  $J = 6.0$  Hz, 3H), 4.96 (q,  $J = 5.9$  Hz, 1H), 6.77 (m, 2H), 7.00–7.13 (m, 21H), 8.00 (m, 12H).  $^{31}\text{P}\{\text{H}\}$  NMR ( $\text{C}_6\text{D}_6$ ):  $\delta$  25.26.  $^{13}\text{C}\{\text{H}\}$  NMR ( $\text{C}_6\text{D}_6$ ):  $\delta$  30.54 (s), 81.28 (t,  $J = 6.2$  Hz), 125.10 (s), 126.03 (s), 127.37 (s), 128.27 (t,  $J = 4.2$  Hz), 130.22 (s), 133.51 (t,  $J = 25.6$  Hz), 135.30 (t,  $J = 6.2$  Hz), 153.22 (s), 175.63 (t,  $J = 11.6$  Hz). IR ( $\text{C}_6\text{D}_6$ ,  $\text{cm}^{-1}$ ): 1945 (s, CO). Anal. Calcd for  $\text{C}_{45}\text{H}_{39}\text{P}_2\text{O}_2\text{Ir}$ : C, 62.44; H, 4.51. Found: C, 62.26; H, 4.44. Complex (**R**)-**6a** was prepared using the general procedure involving reaction of commercial (*R*)-phenethyl alcohol (57.0  $\mu\text{L}$ , 0.473 mmol) with Vaska's complex (200 mg, 0.256 mmol) in the presence of NaH (9.5 mg, 0.40 mmol) to give 126 mg (0.145 mmol, 57%) of enantiopure product.

**trans-[Ir(PPh<sub>3</sub>)<sub>2</sub>](CO)(OCMePh) (6a-d<sub>1</sub>).** Following the general procedure involving alkoxide reagents, Vaska's complex (151 mg, 0.194 mmol) was combined with NaOCMePh (42 mg, 0.290 mmol) in THF. Workup and crystallization from toluene/pentane at  $-35$  °C gave yellow crystals of **6a-d<sub>1</sub>** (100 mg, 0.115 mmol, 59%).  $^1\text{H}$  NMR ( $\text{C}_6\text{D}_6$ ):  $\delta$  0.88 (s, 3H), 6.77 (m, 2H), 7.00–7.07 (m, 21H), 8.00 (m, 12H).  $^{31}\text{P}\{\text{H}\}$  NMR ( $\text{C}_6\text{D}_6$ ):  $\delta$  25.28.  $^2\text{H}$  NMR ( $\text{C}_6\text{D}_6$ ):  $\delta$  4.91.

**trans-[Ir(PPh<sub>3</sub>)<sub>2</sub>](CO)(OCHMe(*p*-C<sub>6</sub>H<sub>4</sub>OMe)) (6b).** Following the general procedure involving alkoxide reagents, Vaska's complex (148 mg, 0.190 mmol) was combined with NaOCHMe(*p*-C<sub>6</sub>H<sub>4</sub>OMe) (51.5 mg, 0.296 mmol) in THF. Workup and crystallization from toluene/

ether mixtures at  $-35$  °C gave yellow crystals of **6b** (102 mg, 0.114 mmol, 60%).  $^1\text{H}$  NMR ( $\text{C}_6\text{D}_6$ ):  $\delta$  0.89(d,  $J = 6.0$  Hz, 3H), 3.38 (s, 3H), 4.96 (q,  $J = 6.0$  Hz, 1H), 6.66 (apparent d,  $J = 8.8$  Hz, 2H), 6.71 (apparent d,  $J = 8.8$  Hz, 2H), 7.0 (m, 18H), 7.19 (d,  $J = 8.3$  Hz, 2H), 8.00 (m, 12H).  $^{31}\text{P}\{\text{H}\}$  NMR ( $\text{C}_6\text{D}_6$ ):  $\delta$  25.07.  $^{13}\text{C}\{\text{H}\}$  NMR ( $\text{C}_6\text{D}_6$ ):  $\delta$  30.73 (s), 54.72 (s), 80.83 (t,  $J = 6.2$  Hz), 112.91 (s), 126.94 (s), 128.27 (t,  $J = 4.6$  Hz), 130.21 (s), 133.56 (t,  $J = 26.8$  Hz), 135.32 (t,  $J = 6.3$  Hz), 145.53 (s), 157.88 (s), 175.70 (t,  $J = 11.6$  Hz). IR ( $\text{C}_6\text{D}_6$ ,  $\text{cm}^{-1}$ ): 1944 (s, CO). Anal. Calcd for  $\text{C}_{46}\text{H}_{41}\text{P}_2\text{O}_3\text{Ir}$ : C, 61.66; H, 4.61. Found: C, 61.62; H, 4.85.

**trans-[Ir(PPh<sub>3</sub>)<sub>2</sub>](CO)(OCHMe(*p*-C<sub>6</sub>H<sub>4</sub>Cl)) (6c).** Following the general procedure involving alkoxide reagents, Vaska's complex (242 mg, 0.310 mmol) was combined with NaOCHMe(*p*-C<sub>6</sub>H<sub>4</sub>Cl) (74.9 mg, 0.419 mmol) in THF. Workup and crystallization from toluene/pentane mixtures at  $-35$  °C gave yellow crystals of **6c** (180 mg, 0.200 mmol, 64%).  $^1\text{H}$  NMR ( $\text{C}_6\text{D}_6$ ):  $\delta$  0.87 (d,  $J = 6.4$  Hz, 3H), 4.85 (q,  $J = 6.0$  Hz, 1H), 6.46 (d,  $J = 8.8$  Hz, 2H), 7.0 (m, 20H), 7.94 (m, 12H).  $^{31}\text{P}\{\text{H}\}$  NMR ( $\text{C}_6\text{D}_6$ ):  $\delta$  25.07.  $^{13}\text{C}\{\text{H}\}$  NMR ( $\text{C}_6\text{D}_6$ ):  $\delta$  30.30 (s), 80.45 (t,  $J = 6.2$  Hz), 127.44 (s), 127.35 (s), 128.29 (t,  $J = 4.5$  Hz), 130.31 (s), 130.49 (s), 133.35 (t,  $J = 25.9$  Hz), 135.23 (t,  $J = 6.0$  Hz), 156.86 (s), 175.42 (t,  $J = 11.1$  Hz). IR ( $\text{C}_6\text{D}_6$ ,  $\text{cm}^{-1}$ ): 1944 (s, CO). Anal. Calcd for  $\text{C}_{45}\text{H}_{38}\text{P}_2\text{O}_2\text{ClIr}$ : C, 60.00; H, 4.22. Found: C, 60.25; H, 4.13.

**trans-[Ir(PPh<sub>3</sub>)<sub>2</sub>](CO)(OCHMe(*p*-C<sub>6</sub>H<sub>4</sub>CF<sub>3</sub>)) (6d).** Following the general procedure involving reaction of alcohol (92.0  $\mu\text{L}$ , 0.60 mmol) with Vaska's complex (150 mg, 0.192 mmol) in the presence of NaH (11 mg, 0.46 mmol), 93 mg (0.100 mmol, 52%) of product was obtained after crystallization from toluene/pentane at  $-35$  °C.  $^1\text{H}$  NMR ( $\text{C}_6\text{D}_6$ ):  $\delta$  0.91 (d,  $J = 6.1$  Hz, 3H), 4.89 (q,  $J = 6.0$  Hz, 1H), 6.57 (d,  $J = 8.3$  Hz, 2H), 7.0 (m, 18H), 7.19 (d,  $J = 8.3$  Hz, 2H), 7.93 (m, 12H).  $^{31}\text{P}\{\text{H}\}$  NMR ( $\text{C}_6\text{D}_6$ ):  $\delta$  25.64.  $^{13}\text{C}\{\text{H}\}$  NMR ( $\text{CD}_2\text{Cl}_2$ ):  $\delta$  29.67 (s), 80.11 (t,  $J = 6.1$  Hz), 123.91 (q,  $J = 4.0$  Hz), 125.68 (q,  $J = 271.6$  Hz), 125.79 (s), 126.71 (q,  $J = 31.3$  Hz), 128.41 (t,  $J = 5.3$  Hz), 130.61 (s), 132.98 (t,  $J = 25.6$  Hz), 135.14 (t,  $J = 5.9$  Hz), 157.24 (s), 175.34 (t,  $J = 11.1$  Hz).  $^{19}\text{F}$  NMR ( $\text{CD}_2\text{Cl}_2$ ):  $\delta$  -60.44. IR ( $\text{C}_6\text{D}_6$ ,  $\text{cm}^{-1}$ ): 1942 (s, CO). Anal. Calcd for  $\text{C}_{46}\text{H}_{38}\text{P}_2\text{O}_2\text{F}_3\text{Ir}$ : C, 59.16; H, 4.10. Found: C, 58.99; H, 4.03.

**Kinetic Measurements of  $\beta$ -Hydrogen Elimination from Iridium Alkoxides in  $\text{C}_7\text{D}_8$  and Data Processing.** A stock solution consisting of 0.0050 M iridium alkoxide was prepared in toluene-*d*<sub>8</sub> and stored in a  $-35$  °C freezer. A typical reaction mixture was prepared by mixing 0.65 mL of the stock solution with 3.6 mg (0.013 mmol, 0.020 M) to 54 mg (0.19 mmol, 0.30 M) of PPh<sub>3</sub>-*d*<sub>15</sub>. The  $\beta$ -hydrogen elimination was monitored by proton NMR spectroscopy at 95 or 108 °C. The spectra were measured using 5-mm screw-capped NMR tubes, which were inserted into a pre-shimmed and pre-warmed NMR spectrometer probe. An automated acquisition program was started after 4–5 min of temperature equilibration. The reactions were monitored for at least three half-lives. Raw data from the spectra were processed using the KaleidaGraph program on a Macintosh personal computer.

**Evaluation of Alkoxide Racemization.** A 5-mm screw-capped NMR tube was charged with a solution containing 5.6 mg (0.0065 mmol, 0.0050 M) of complex (**R**)-**6a** and 102 mg of PPh<sub>3</sub> (0.389 mmol, 0.300 M) or 6.8 mg of PPh<sub>3</sub> (0.026 mmol, 0.020 M) in 1.3 mL of toluene. The sample tube was capped with a septum. The tube was placed into a 100 °C oil bath. The reaction was monitored by  $^{31}\text{P}$  NMR spectrometry. Three or four aliquots of roughly 0.3 mL volume were removed at different conversions of alkoxide complex. Each sample was hydrolyzed by addition of excess water, and the enantiomeric excess of the free alcohol was then determined by chiral capillary GC or chiral stationary phase HPLC. Identical enantiomeric excess was obtained by chiral capillary GC without the hydrolysis step.

**Acknowledgment.** We thank the PRF for partial support of this work, along with the DOE. We are also grateful to Johnson-Matthey for a gift of IrCl<sub>3</sub>·3H<sub>2</sub>O. We thank Prof. Jack Faller for helpful comments on the stereochemical requirements for alkoxide racemization.